

Digital Receiver Design for an Offset IF LFM-CW SAR

Craig Stringham and David G Long
 BYU Microwave Earth Remote Sensing Laboratory
 Provo, Utah
 stringham@mers.byu.edu and long@ee.byu.edu

Brandon Wicks and Glenn Ramsey
 ARTEMIS, Inc.
 Hauppauge, New York
 bwicks@artemisinc.net and gramsey@artemisinc.net

Abstract—This paper describes the digital receiver for the microASAR, a small, powerful, LFM-CW SAR. The digital receiver uses a high-speed ADC providing three key benefits; namely: 1) the de-chirped signal can be at an arbitrary intermediate frequency (IF), enabling better RF filtering; 2) quantization noise can be reduced via digital filtering; and 3) the flexibility to enable the SAR to operate in both de-chirped and pulsed modes. This paper also outlines the FPGA design used for most applications.

I. INTRODUCTION

In 2005, the Microwave Earth Remote Sensing (MERS) lab at Brigham Young University (BYU) developed the microSAR, demonstrating a small and low-cost LFM-CW SAR system [1]. Building on this experience, BYU partnered with Artemis Inc. to develop the microASAR, a more robust and capable system, that overcomes many of the limitations of the microSAR design [2]. A key feature of the microASAR design is an oversampled digital receiver. The oversampling provides three main benefits, namely: the de-chirped signal can be at an arbitrary intermediate frequency (IF), enabling better RF filtering; quantization noise is reduced via digital filtering; and the flexibility to enable the SAR to operate in both de-chirped and pulsed modes. In this paper we briefly describe the design and results of this system.

II. BACKGROUND - TRADITIONAL LFM-CW SAR

An LFM-CW SAR is designed to achieve maximum signal to noise ratio (SNR), improving image quality for a given transmit power level. This is accomplished by continuously transmitting a frequency modulated chirp. Fig. 1 shows a high-level flow diagram for a typical homodyne LFM-CW SAR system. A frequency modulated chirp is generated via a direct digital synthesizer (DDS) and mixed up to a carrier frequency and transmitted. Unlike a traditional pulsed SAR system, an LFM-CW SAR receiver is on during transmit, typically using a separate antenna. The non-ideal isolation of the physical transmit and receive channels (in the RF system and the antennas) introduces a feed-through component that dominates the radar echoes.

To reduce the bandwidth of the echoes, the received signal is “de-chirped”. Dechirping consists of mixing the received signal with the transmit signal. Filtering the feedthrough component requires a high-Q filter as the feed-through component

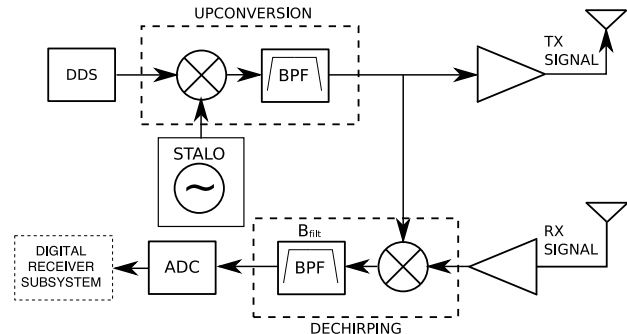


Fig. 1: (a) A high-level flow diagram and a typical homodyne LFM-CW SAR system.

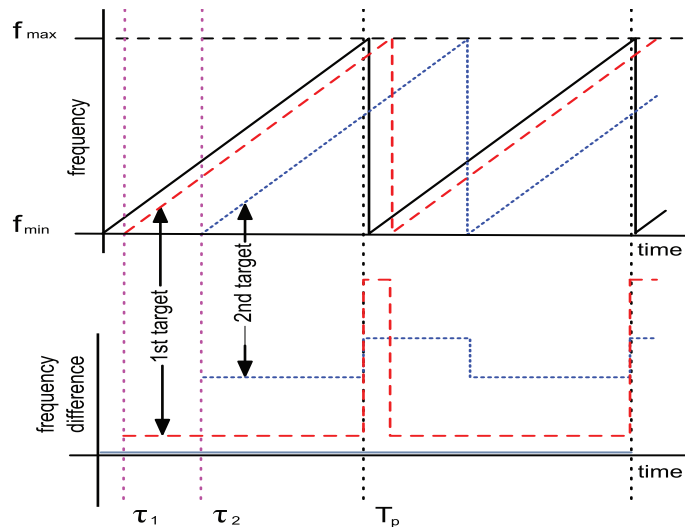


Fig. 2: A time frequency representation of LFM-CW operation and the de-chirped signal.

is near DC and separated from the echoes by an audio frequency, approximately equal to the product of the chirp-rate and the range time of the nearest target.

Fig. 2 illustrates the de-chirping time versus frequency. The transmit chirp, represented by the solid line, starts at the minimum frequency linearly increasing, as determined by the chirp rate (k_r), up to the maximum frequency and then repeating. The echoes are copies of the transmit signal

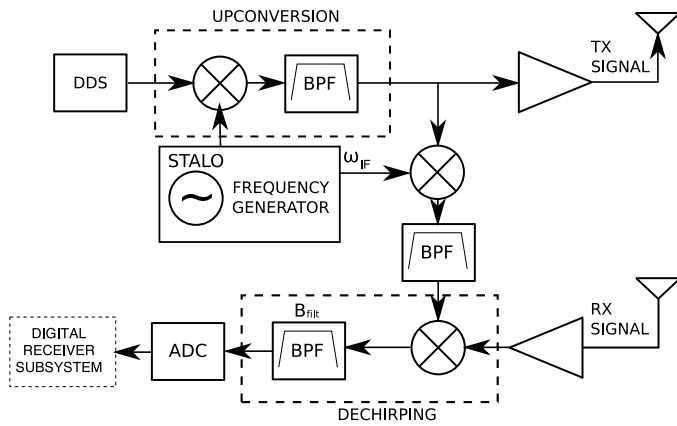


Fig. 3: (a) A high-level flow diagram for an offset IF homodyne LFM-CW SAR. The received signal is mixed down with a frequency shifted version of the transmit signal. The resulting signal is at an offset IF. The higher IF center frequency enables the use of a better filter without distorting the signal.

occupying the same range of frequencies but are delayed in time. The process of de-chirping translates the time delay into a frequency difference, as shown in the lower portion of Fig. 2. In selecting the bandpass filter that sufficiently suppresses the feed through, a wider cutoff region may be accepted by increasing the ramp rate to increase the separation of the feed-through and the echoes. A higher ramp-rate increases the bandwidth of the signal, and thus to maintain a lower data rate the data is presumed as explained later.

III. OFFSET IF LFM-CW SAR

The previous derivation is the basis for the BYU microSAR, which worked adequately, but it was found that the high-Q filter used to suppress the feed-through causes distortion to the echo data due to the filter's long impulse response. This distortion can be avoided using an offset de-chirp. We term this system an offset IF LFM-CW SAR.

The flow diagram for an offset IF LFM-CW SAR is shown in Fig. 3. To generate the dechirp signal, the transmit signal is first partially mixed down using ω_{IF} and filtered. This signal is then mixed with the received signal, the resulting difference components are similar to the ones in the traditional LFM-CW but are at an offset IF. With the signal of interest at a higher IF frequency, it is easier to find a high-Q filter that has linear phase, sharp cutoff frequencies, and better suppresses the feed-through.

IV. DIGITAL IF DESIGN

The design of the digital receiver for offset IF LFM-CW SAR system can follow traditional LFM-CW receiver design if another mix down stage is added to mix down the offset dechirp signal or if the sampling frequency and analog to digital converter (ADC) are carefully selected to sub-sample the offset dechirp signal; however, improved performance and flexibility can be achieved when using a high-speed ADC and an FPGA. Choosing an ADC that can sample the full

bandwidth of the received chirp enables pulse mode operation as well as dechirp operation at an arbitrary IF. Incorporating an FPGA further enhances the design by providing enough I/O ports to integrate a large number of components and communication devices. The FPGA provides for various modes of operation. This section describes the principles of oversampling and filtering used in implementing the microASAR. The FPGA implementation is described in the next section.

A. Oversampling

When the relative power consumption costs can be neglected and the ADC resolutions are comparable, it is best to sample the received signal at the highest rate possible to enable quantization noise reduction. Because the quantization noise is independent of sampling frequency, sampling the signal at a higher rate spreads the noise spectrum over a wider bandwidth and thereby lowers the quantization noise power over the signal bandwidth.

Introductory digital signal processing courses often neglect the effects of amplitude quantization; however, in a LFM-CW system the quantization of the incoming signal is often the major source of noise. When a sufficiently random signal is quantized at a step size q , it is equivalent to the addition of uniform white noise in the range of $\pm \frac{q}{2}$ (see [3]). By applying an appropriate filter after sampling the signal, the quantization noise ratio (QSNR) is increased by approximately 3dB for every factor of 2 the signal is oversampled.

Fig. 4 illustrates the SNR benefit available by oversampling. In Fig. 4a a simulated LFM-CW echo is sampled at a rate just above Nyquist. The separation between the signal and the quantization noise is about 64dB. The signal in Fig. 4b is oversampled by a factor of approximately 18 with the same number of bits as in Fig. 4a. The separation between the signal and noise is now about 75dB. By appropriately applying a bandpass filter, oversampling enables a 11dB QSNR increase.

B. Data Rate Reduction

Once the signal is sampled, the next step is to reduce the data rate without compromising the integrity of the data. There are two steps in the process. The first is to filter the quantization noise and bring the signal to baseband such that the filtered signal sampling frequency can be reduced. All of the filters implemented are digital polyphase filters, which combine the operation of a filter and a decimator enabling a reduction in FPGA resources. The second step in reducing the data rate is presumming. Presumming consists of adding sequential echoes together and has the effect of low pass filtering the Doppler spectrum. Presumming can be used on the microASAR data because the high PRF used to separate the feed-through and the first target, as explained in Sec. III, is much higher than required by the Doppler bandwidth of the signal.

The order of the presumming and filtering are interchangeable from a signal processing point of view, but the order greatly affects the memory and hardware requirements of the implementation, as discussed in the following section. Also it

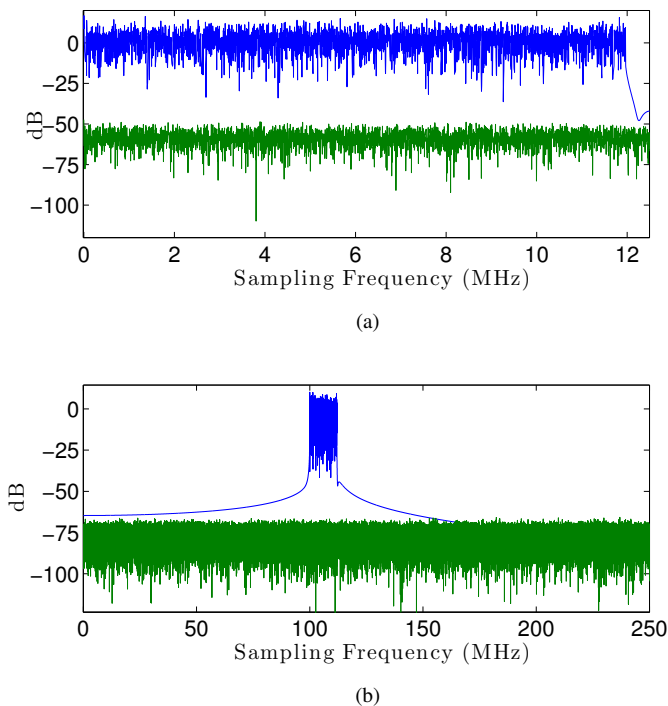


Fig. 4: Plots depicting the spectrum of the subsampled(a) and oversampled(b) signal with the respective quantization noise. Note that the oversampled signal has a larger signal to noise separation of approximately 11dB. Note that the signal spectrum has the same bandwidth in both plots but the frequency scaling of the plots is different.

should be noted that after every signal processing operation the bitwidth of the data path is increased to prevent overflow [4].

V. FPGA IMPLEMENTATION

In order to achieve the desired system flexibility and high performance obtainable using the principles described in the previous section, the microASAR digital receiver is equipped with a 12-bit 500MHz ADC and a Xilinx Virtex FX FPGA. This combination enables the microASAR to sample the full 200MHz bandwidth of the transmitted signal as well as operate in various dechirp modes. This section briefly describes the general design of the FPGA implementation for dechirp operation and outlines the design strategy used.

The general outline of the FPGA implementation is shown in Fig. 5. The embedded PowerPC processor on the FPGA is used to control and coordinate the operation of the complete digital receiver, and most operational parameters can be set by communicating with the powerPC via ethernet. The normal signal data path goes from the ADC to the filter subsystem and then through a buffer to the compact flash cards. Alternatively, the data path can be interrupted and streamed across the ethernet port. The data from the ADC is immediately broken into two interleaved data paths such that the filter clock rate can be reduced by a factor of two to ease timing constraints.

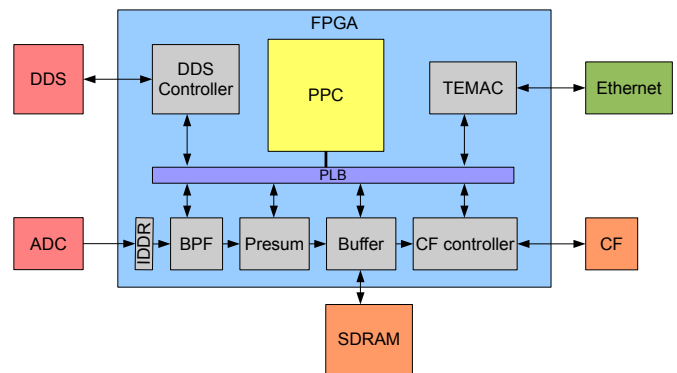


Fig. 5: Block diagram of the FPGA implementation. Note that the order of signal data path can change depending on design parameters.

The two data streams are 180 degrees out of phase with each other and are recombined following the presum stage.

The filter subsystem includes all the filtering, presuming, and decimation steps, and can be configured for differing operational parameters. In order to handle a large range of operations and to reduce FPGA resources, the filter subsystem consists of a polyphase filter followed by the presumer. The polyphase filter reduces quantization noise and limits the signal spectrum such that the signal can be translated to DC by decimating the digitally sampled data. For the microASAR this is done by applying a 12MHz wide BPF starting at the ω_{PF} and decimating by a factor of 20, providing approximately 2.3 bits of increased resolution. The presuming is performed after the filter in order to reduce memory requirements so that presuming can be computed in on-chip memory.

Alternatively, performing presuming first reduces the multipliers required in filtering. In most cases though, this requires an external high-speed memory, increasing power consumption and development time. Replacing the single polyphase filter with a polyphase filter followed by a mixer and a polyphase low pass filter enables a larger bandwidth to be stored and the “empty” spectrum due to the distance from the SAR to the nearest target to be discarded. Also, instead of the mixer and low-pass filter an FFT could be used. Both of these methods require more FPGA resources and add noise to the signal due to the fixed point multiplies and sine/cosine lookup tables.

This simple setup minimizes the FPGA resources and can be operated for a variety of applications simply by varying the PRF. Decreasing the PRF decreases the chirp rate, compressing the targets in the dechirped data. The analog and digital filters effectively range gate the dechirped data. So by varying the PRF from 7-14 kHz the SAR can be operated with altitudes of 5-1000 m, a maximum swath width of 30-2500 m, and a velocity of 0-150 m/s. For a more detailed explanation see [2]. Some values of these parameters are obviously impractical for airborne operation, but the microASAR can be used for ground based systems as well.

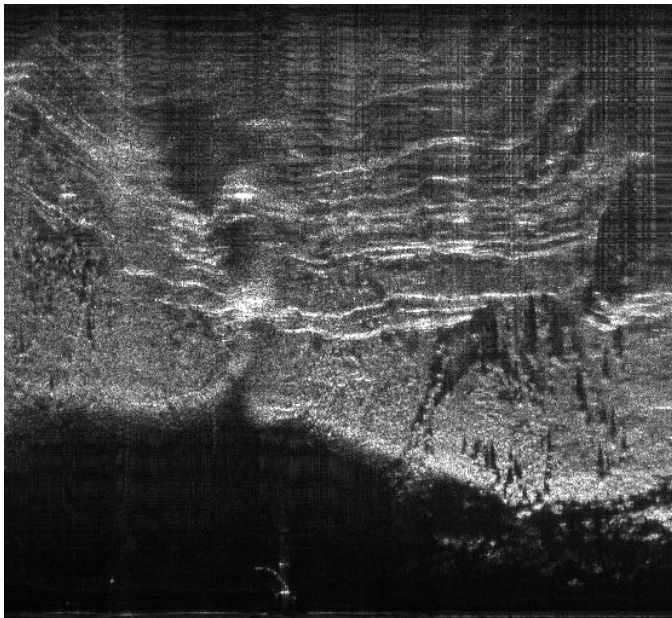


Fig. 6: SAR image collected of Provo Canyon using the microASAR on the side of a car.

VI. RESULTS

Initial tests were performed using evaluation boards bootstrapped to the analog hardware, while a custom board was being designed. The first test of the hardware was done using an optical delay line. Afterwards a “road test” was made using the microASAR by attaching the antennas to the side of a car to image a canyon wall from a highway. Fig. 6 is an image collected using a portion of the data collected. The car is travelling at the bottom of the image from right to left. The black region at the bottom is due to a ravine next to the road. The trees in the lower portion of the image focused well, and the sedimentary rock folds of the canyon wall are clearly visible. The defocusing in the far range is due to the changing topography of the canyon and the curvature of the road.

After the road tests several tests were completed using a variety of small airplanes and UAVs. Fig. 7 is an example of

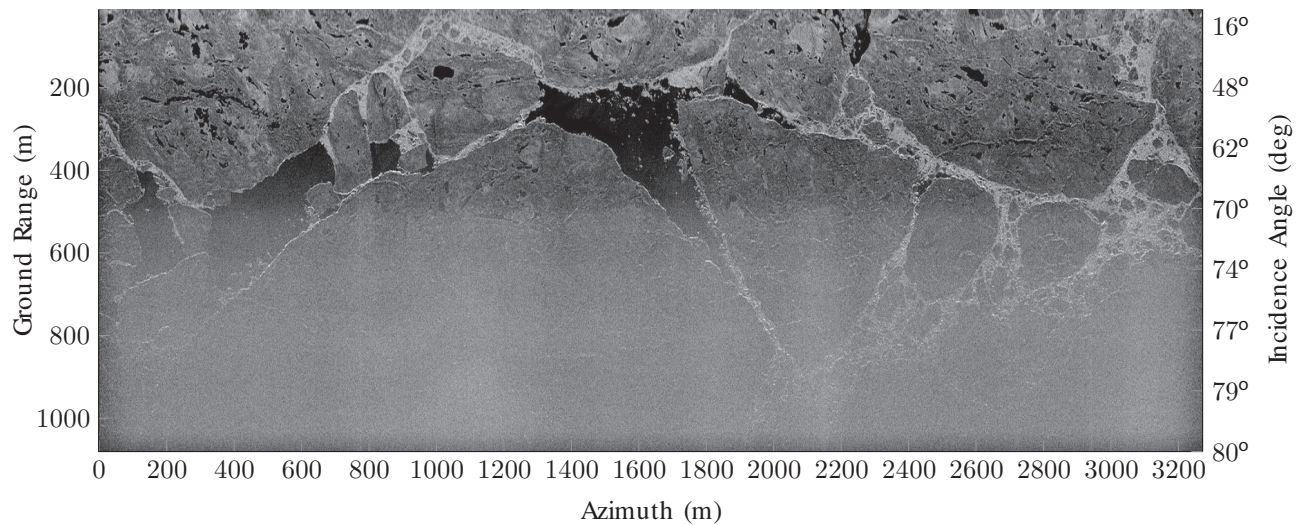
the imagery created using data collected with the microASAR over the Arctic ocean during the characterization of sea ice experiment (CASIE) in 2009 [5], [6]. The ice edges and ice flows are easy to discriminate. Note that these images are collected at low altitudes such that the incidence angle varies greatly in the across track direction. The higher incidence angle causes a lower return from the sea ice, so a linear scaling factor has been applied to the images to normalize the contrast. This makes the lower parts to appear noisier. This is due to the lower return caused by the distance and incidence angle.

VII. CONCLUSION

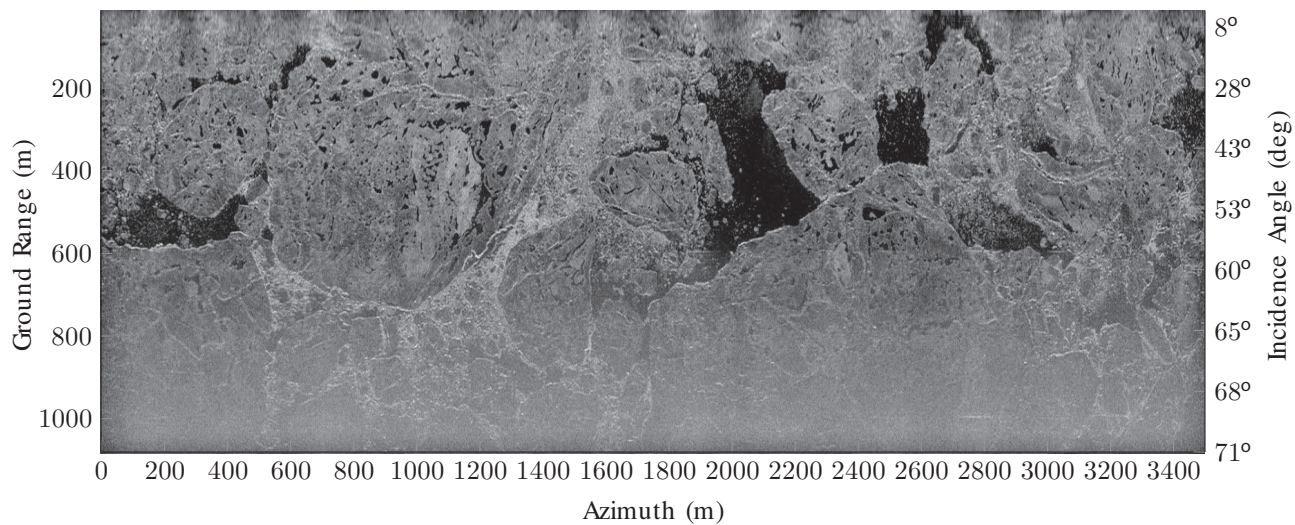
This paper has described the motivation and design of an offset IF LFM-CW digital receiver using a high-speed ADC and an FPGA. The offset dechirp enable the use of better analog filters. The oversampling design allows for the dechirped signal to be at an arbitrary IF and for quantization noise to be reduced with the application of appropriate digital filters. As the images from this system show, the microASAR can be an effective tool for a variety of scientific and military applications.

REFERENCES

- [1] E. Zaugg, D. Hudson, and D. Long, “The BYU SAR: A small, student-built SAR for UAV operation,” in *IEEE International Conference on Geoscience and Remote Sensing Symposium, 2006. IGARSS 2006, 2006*, pp. 411–414.
- [2] M. Edwards, D. Madsen, C. Stringham, A. Margulis, B. Wicks, and D. Long, “microASAR: A small, robust LFM-CW SAR for operation on UAVs and small aircraft,” in *Geoscience and Remote Sensing Symposium, 2008. IGARSS 2008. IEEE International*, vol. 5, July 2008.
- [3] B. Widrow and I. Kollar, *Quantization noise*. Cambridge University Press, 2008.
- [4] C.-Y. Chi, D. Long, and F.-K. Li, “Roundoff noise analysis for digital signal power processors using Welch’s power spectrum estimation,” *Acoustics, Speech and Signal Processing, IEEE Transactions on*, vol. 35, no. 6, pp. 784 – 795, jun 1987.
- [5] E. Zaugg, D. Long, M. Edwards, M. Fladeland, R. Kolyer, I. Crocker, J. Maslanik, U. Herzfeld, and B. Wallin, “Using the MicroASAR on the NASA SIERRA UAS in the Characterization of Arctic Sea Ice Experiment,” in *Radar Conference, 2010 IEEE*, May 2010, pp. 271 – 276.
- [6] D. G. Long, E. Zaugg, M. Edwards, and J. Maslanik, “The microASAR experiment on CASIE-09,” in *Geoscience and Remote Sensing Symposium (IGARSS), 2010 IEEE International*, Jul. 2010, pp. 3466 –3469.



(a)



(b)

Fig. 7: Example imagery obtained using the microASAR, an offset IF LFM-CW SAR system.